UNIVERSIDADE DE SÃO PAULO

INSTITUTO DE FÍSICA
CAIXA POSTAL 20516
01498 - SÃO PAULO - SP
BRASIL

publicações

IFUSP/P-446

CORRELATION BETWEEN CHARGED-PARTICLE MULTIPLICITIES AND PSEUDO-RAPIDITY DISTRIBUTIONS IN HYDRODYNAMICAL CLUSTER MODEL

by

Y. Hama and F.S. Navarra
Instituto de Física, Universidade de São Paulo

Dezembro/1983

CORRELATION BETWEEN CHARGED-PARTICLE MULTIPLICITIES AND PSEUDO-RAPIDITY DISTRIBUTIONS IN HYDRODYNAMICAL CLUSTER MODEL

Y. Hama and F.S. Navarra

Instituto de Física, Universidade de São Paulo
C.P. 20516, 01498 São Paulo, SP, Brasil

ABSTRACT

It is shown that the correlation between charged-particle multiplicities and pseudo-rapidity distributions, such as the one observed in ISR as well as in recent $\bar{p}p$ collider experiments may well be understood in terms of the previously studied hydrodynamically-expanding large-cluster model.

1. The multiplicity dependence of the particle distribution in pp collisions had been obtained at the ISR by Thomé et al. [1]. The essential feature of those data was the double-bumped structure of the η-distributions at low multiplicities, suggesting fragmentation of the incoming protons, and the disappearance of these peaks as n increased. Recent experiments at the $\bar{p}p$ collider [2,3] have confirmed the persistence of this behaviour at higher energies and moreover shown that as n increases the peaks move toward smaller values of $|\eta|$ (or there develop new bumps in the plateau region as interpreted by the authors of Ref. [2]). The data mentioned above seem us to be somewhat conflicting about this point.

Besides the semi-inclusive distributions reported in the above papers, another experiment [4] has shown that, in these collisions, the final particles appear in general distributed with respect to the center of mass in a highly asymmetric way*. Although it is possible to interpret this asymmetry as due to fluctuations, if a random small-cluster emission is assumed [4], we shall prefer to adopt an alternative interpretation by which the asymmetry is due to a formation of large-mass clusters (as will be explained in the next sections), which appear asymmetrically in the center-of-mass system. That is, we interpret these data as showing a definite tendency of the produced particles to select either the forward or the backward direction, forming large clusters.

---

*See especially Fig. 1 of the present paper, where we have reproduced the data shown in Fig. 4 of [4].

2. In a previous work [5], we have studied the correlation between $\langle p_\perp \rangle$ and the central multiplicity and compared with the recent collider's data [6], by using a model in which one or two large-mass fireballs are formed. The description of these (initially pancake shaped) fireballs is given [7] within the usual hydrodynamical model [8] and their transverse expansion would cause the increase of $\langle p_\perp \rangle$ as the fireball mass M increases (and so does the multiplicity n). The point is that M is not fixed and it varies from event to event, so that, for large-M events, both $\langle p_\perp \rangle$ and n are on the average large. Recently published ISR data [9] confirm our prediction, except for the extreme low multiplicity points*. In the present paper, we shall therefore apply the same idea above for the study of the longitudinal distribution and see whether the model is still useful in order to understand the main empirical features mentioned in 1.

3. Assume, then, that during a collision between two hadrons ($\bar{p}$ and p to fix the idea), hot blobs are excited around one or both of the incident particles. As explained in [7], this assumption together with the equation of state (we assume here $p = \frac{\varepsilon}{3}$) allow us to establish a definite relation between the mass of the fireball M in one hand and the thermodynamic quantities such as the initial temperature and the entropy on the other hand. The existence and the

*We think these points are in conflict with the well known inclusive $\langle p_\perp \rangle$, which is much smaller. See, for instance, [10], where the data are parametrized $E \frac{d\sigma}{d\vec{p}}\Big|_{\frac{\pi}{2}} \propto \exp\left[-B\sqrt{p_\perp^2+m^2}\right]$, with $B = 7.1 \sim 7.2$ GeV^{-1}.

dominance of such a mechanism of production (illustrated by Fig. 2) are supported by the results we have already reported [7,11] and moreover give a simple explanation of the forward-backward asymmetry mentioned above. Although we do not exclude other possibilities, this is also a natural way to separate the leading particle as discussed in [7], giving a simple description of the rest of the system. In our model, only one leading particle may appear in each event, which in our opinion is not in contradiction with the existent data.

Consider a cluster of mass M. Following Ref. [5], the average charged multiplicity is

$$\langle n_{ch} \rangle (M) \cong 2.2 \sqrt{M} \quad . \tag{1}$$

As stressed in 2, M is not fixed, but varies from event to event and so does $\langle n_{ch} \rangle (M)$. So, once n_{ch} is fixed*, we may in first approximation (we neglect all the fluctuations in n_{ch}) determine the corresponding M and then compute $d\sigma/d\eta$. As in [5], we assume factorized particle distribution

$$\frac{dn}{dy\, d^2\vec{p}_\perp} = f(\sqrt{s},M,y)\, g(M,p_\perp) \quad , \tag{2}$$

where, according to hydrodynamical model,

$$f(\sqrt{s},M,y) \cong \frac{\langle n_{ch} \rangle (M)}{\sqrt{\pi L_M}} \exp\left[-\frac{(y-y_M)^2}{L_M}\right] \quad , \tag{3}$$

*In the actual calculation, we took into account that the measured n_{ch} is not the total charged multiplicity, but that η-interval is restricted.

with $\begin{cases} y_M \cong \ell n \frac{\sqrt{s}}{M} \quad , \quad \text{(center of mass of the cluster)} \\ L_M \cong 2.24\, \ell n\, M + 2.56 \quad . \end{cases}$ (4)

Here, following Milekhin's result [12], which takes the transverse expansion into account, we have slightly changed L_M as compared with the value we have used in [5]. This modification, however, does not change the results reported there in any considerable amount.

As for the transverse part $g(M,p_\perp)$, instead of the assumption $\xi = \langle\xi\rangle$ as in [5], we parametrize it in a more realistic (exponential) form

$$g(M,p_\perp) = \frac{1}{\pi C^2 m_\pi^2 M^{2/7}} \exp\left[-\frac{2p_\perp}{C m_\pi M^{1/7}}\right] , \qquad (5)$$

which is normalized and gives mikekhin's result [12]

$$\langle p_\perp\rangle \cong C m_\pi M^{1/7} \exp\left[-\frac{(y-y_M)^2}{3L_M}\right] \cong C m_\pi M^{1/7} , \qquad (6)$$

with

$$C \cong \frac{0.53}{(2m_p)^{1/14}} . \qquad (7)$$

In (6), for the sake of simplicity we have neglected a slowly varying y-dependent factor.

4. We are now ready to compute everything we need by using the ingredients given in the preceding section. In doing so, recall that all the available data [1-4] are referred to η

and not to y. Although these variables are almost identical, some differences appear between two descriptions, especially in the central region [13]. Probably, the two-bump structure which is seen in the very-large multiplicity data on $d\sigma/d\eta$ and reported in [2] as a new characteristic of these phenomena is due to the use of η instead of y, with respect to which the distribution would be flat, or even with a peak at $y = 0$. The explicit inclusion of $p_\perp$ dependence in eqs. (2,5) is precisely to account for this effect. Instead of a direct comparison $dn/dy \cong dn/d\eta$ as given by (3), we rewrite it in terms of η, integrate it to obtain $\frac{dn}{d\eta}$ and then compare with the data.

5. Forward-Backward Asymmetry. One of the characteristics of our model is the strong forward-backward asymmetry in the particle distribution. This is especially so, if one-cluster events, Fig. 1(a,b), are dominant, but it also manifests in the case of two-cluster events, since presumably $M_1 \neq M_2$ in the most of these events.

In Ref. [4], charged particles produced in $\bar{p}p$ collider had been detected in the two intervals $1 < |\eta| < 4$ and the events classified according to the forward and the backward multiplicities n_F and n_B. In Fig. 1, the forward-backward distribution is plotted for a fixed value of $n_S \equiv n_F + n_B$. In order to compare our model with these data, we have computed the distributions corresponding to the two extreme cases, namely i) when all the contributions come from equal-mass double-cluster term, Fig. 1(c) with $M_1 = M_2$ (which gives the binomial distribution); and ii) when all the contributions come from one-cluster term, either Fig. 1(a)

or (b). The corresponding mass in the case of $n_s = 12$ is $M = 96$ GeV and the distribution has been computed by assuming a random production of particles with the probability in each pseudo-rapidity interval $\Delta\eta$ given by

$$P(\Delta\eta) \propto \int_{\Delta\eta} \frac{dn}{d\eta}\, d\eta \quad . \tag{8}$$

It is clear from Fig. 1 that, for this multiplciity, neither of the extreme cases gives a quantitative agreement with the data, but some 50% mixture may give a nice account of them.

6. Semi-Inclusive Pseudo-Rapidity Distributions. From the discussion above, it becomes apparent that the one-cluster or else the two-unequal-cluster formation plays an important rôle in our model. At this point, a word of remark is in order. As explicitly stated in Refs. [2] and [3], the trigger condition in those experiments was such that at least one charged particle was required in coincidence in each of the hemispheres. So, at first sight, one-cluster events would be completely excluded, but a detailed analysis shows that this is not so. Following the experimental condition stated in [3], we have verified that if a cluster of mass $M \geq 44$ GeV is formed in the forward direction, then $n_{ch}(\eta < -1.6) \geq 1$, which means that almost all of these events have been detected. If one considers that the above bound corresponds to $n_{ch}(|\eta| < 3.5) \simeq 7.9$ and looks at Fig. 3, one realizes that only in the lowest-multiplicity case the required condition is not satisfied by the majority of the events.

We are now ready to compare the predictions of the

model with the data. In Fig. 3, we have plotted several curves computed on the assumption of the one-cluster dominance. If one includes also the two-cluster events, the peaks move slightly to higher values of η. As we have, at the present, no explicit formula giving the mass distribution for the two-cluster events, we are not going to compute these curves here. Coming back to Fig. 3, one sees clearly that the main experimental features are well reproduced both qualitatively and quantitatively. Observe that although the maximum of $f(\sqrt{s},M,y)$ for $M = 360$ GeV is at $y = 0.41$ according to eq. (4) and so probably at $y \simeq 0$ in the final semi-inclusive $\frac{dn}{d\eta}$, it appears at $\eta \simeq 1.7$ in Fig. 3, confirming what has been said in 4.

7. To conclude this paper, we summarize the results obtained so far, by using our simple model. First, it has supplied a very nice overall description of the large missing-mass clusters, yielding the average multiplicity $\langle n_{ch} \rangle (M)$, the multiplicity distribution as a function of M and the rapidity distributions for fixed M, all of them in agreement with the data [7,11]. When the transverse expansion has been taken into account, it has shown the correct multiplicity - $\langle p_\perp \rangle$ correlation [5]. Now, from the discussion above, we conclude that it exhibits also the gross features of the pseudo-rapidity distributions for fixed charged multiplicities n_{ch}.

Some problems which have to be solved to go one step further should be mentioned here. First, the mechanism of fireball excitation has not been so far studied in a satisfactory way. In our opinion, it is not reasonable (in hadron-hadron

collisions) to treat the process of the initial hot blob formation in a classical geometrical way. Quantum fluctuations must somehow play an important rôle in this process, being the semi-classical treatment justified only in the phase of the fireball expansion. Such fluctuations would give a broad fireball mass distribution, originating events of variable multiplicities. The exact form of the mass spectrum should be determined, at least on the phenomenological basis. A related question is the multiplicity distribution. Finally, as stated below eq. (1), we have neglected the multiplicity fluctuation for fixed M, computing everything with $\langle n_{ch} \rangle$. This has evidently caused effects similar to these mentioned in the foregoing paper [5], where we had data points with the multiplicity larger than the maximum value of $\langle n_{ch} \rangle$ predicted by eq. (1). While conceptually no difficulty is posed here and their qualitative behaviour is reasonable, a quantitative treatment of these data depends on many parameters and is not easy.

The authors acknowledge that the present work has been initiated while one of them [Y.H.] was visiting CERN's TH Division within the framework of the CNPq-CERN agreement. He is especially indebted to L. Van Hove for stimulating discussions.

REFERENCES

[1] W. Thomé et al., Nucl. Phys. B129 (1977) 365.

[2] K. Alpgård et al., Phys. Lett. 107B (1981) 315.

[3] G. Arnison et al., Phys. Lett. 123B (1983) 108.

[4] K. Alpgård et al., preprint CERN-EP/83-20 (1983).

[5] Y. Hama and F.S. Navarra, Phys. Lett. 129B (1983) 251.

[6] G. Arnison et al., Phys. Lett. 118B (1982) 167.

[7] Y. Hama, Phys. Rev. D19 (1979) 2623.

[8] L.D. Landau, Izv. Akad. Nauk SSSR Ser. Fiz. 17 (1953) 51; Collected papers, ed. D. Ter Haar (Pergamon, Oxford, 1965) p. 569.

[9] A. Breakstone et al., Phys. Lett. 132B (1983) 463.

[10] K. Guettler et al., Phys. Lett. 64B (1976) 111.

[11] Y. Hama and F.W. Pottag, Rev. Bras. Fis. 12 (1982) 247.

[12] G.A. Milekhin, Sov. Phys. JETP 35 (1959) 829.

[13] Y. Hama, Jour. Phys. Soc. Japan 50 (1981) 21.

FIGURE CAPTIONS

Fig. 1 – The forward-backward distribution for 185 events with $n_S \equiv n_F + n_B = 12$ in $\bar{p}p$ collisions at 540 GeV. n_F and n_B are respectively the numbers of the forward and the backward charged secondaries in the pseudo-rapidity intervals $1 < |\eta| < 4$. The curves are explained in the text.

Fig. 2 – Diagramatic representation of the model explained in 3.

Fig. 3 – Normalized pseudo-rapidity distributions for various charged multiplicities, predicted by one-cluster model. The mass values are from the bottom to the top: M = 18, 50, 140 and 360 GeV. The data compared are from Refs. [2,3].

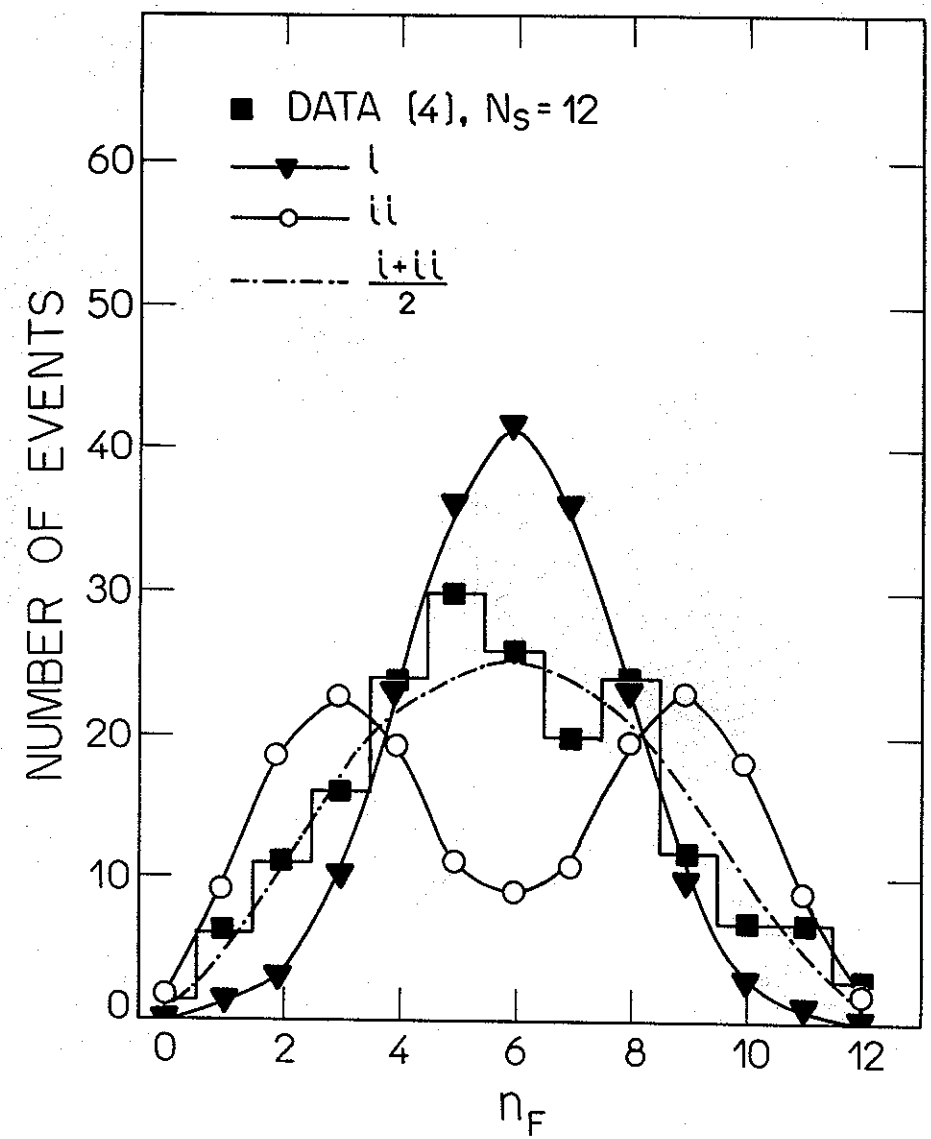
DATA (4), $N_S = 12$
I
II
$\frac{I+II}{2}$
NUMBER OF EVENTS
n_F
0
10
20
30
40
50
60
0
2
4
6
8
10
12

Fig.1

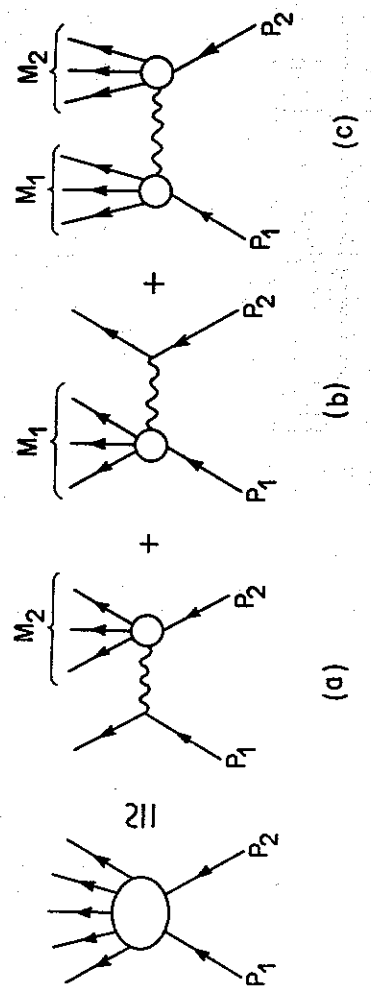
M_2
P_2
M_1
P_1
(c)
+
M_1
P_2
P_1
(b)
+
M_2
P_2
P_1
(a)
=
P_2
P_1

Fig. 2

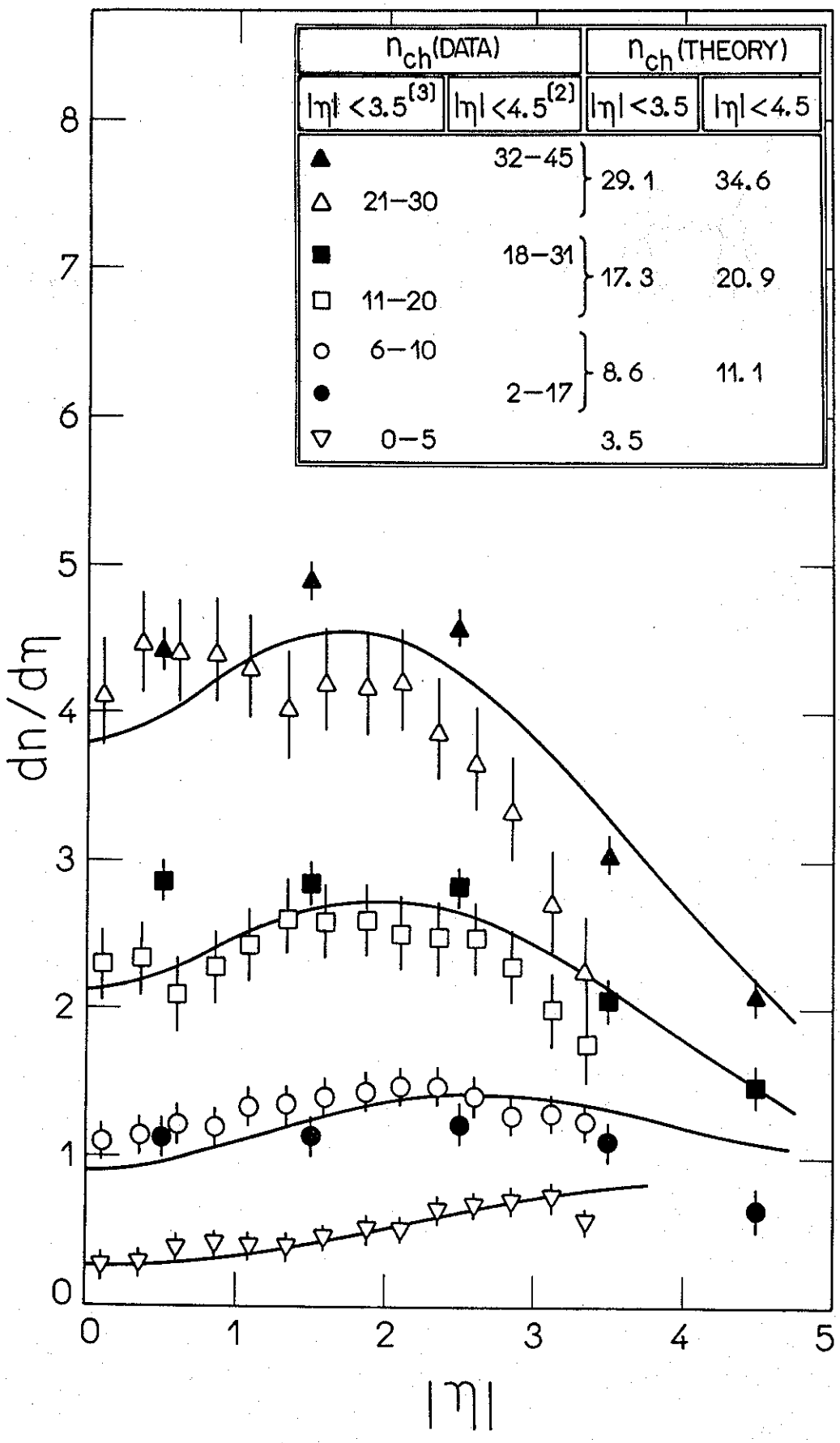
n_{ch}(DATA)
n_{ch} (THEORY)
$|\eta| < 3.5$[3]
$|\eta| < 4.5$[2]
$|\eta| < 3.5$
$|\eta| < 4.5$
32–45
21–30
29.1
34.6
18–31
11–20
17.3
20.9
6–10
2–17
8.6
11.1
0–5
3.5
dn/dη
|η|
0
1
2
3
4
5
6
7
8

Fig. 3